EFFECT OF FIBER-REINFORCED CEMENT COMPOSITES ON THE SEISMIC PERFORMANCE OF BRIDGE COLUMNS

Richelle G. ZAFRA[1] · Tomohiro SASAKI[2] · Kazuhiko KAWASHIMA[3] · Koichi KAJIWARA[4] and Manabu NAKAYAMA[5]

[1] Graduate Student, Department of Civil Engineering, Tokyo Institute of Technology (2-12-1 O-okayama, Meguro, Tokyo 152-8552, Japan)
[2] Member of JSCE, Graduate Student, Department of Civil Engineering, Tokyo Institute of Technology (2-12-1 O-okayama, Meguro, Tokyo 152-8552, Japan)
[3] Member of JSCE, Professor, Department of Civil Engineering, Tokyo Institute of Technology (2-12-1 O-okayama, Meguro, Tokyo 152-8552, Japan)
[4] Member of JSCE, Senior Researcher, Hyogo Earthquake Engineering Research Center, National Research Institute for Earth Science and Disaster Prevention (1501-21 Nishikameya, Mitsuta, Shijimi-cho, Miki, Hyogo 673-1505, Japan)
[5] Member of JSCE, Research Fellow, Hyogo Earthquake Engineering Research Center, National Research Institute for Earth Science and Disaster Prevention (1501-21 Nishikameya, Mitsuta, Shijimi-cho, Miki, Hyogo 673-1505, Japan)

1. INTRODUCTION

Bridges are important structures that require a high degree of protection to ensure their functionality after a seismic event. To allow for energy dissipation during an earthquake, damage to plastic hinges is accepted. The damage, however, may render the structure unusable after an earthquake and may interfere with disaster recovery operation. Thus, column plastic hinges that can dissipate energy without experiencing severe damage can alleviate these problems.

Materials that undergo substantially reduced damage while dissipating energy under severe seismic loading are desired. Fiber reinforced cement composites (FRCC) is a class of high-performance material that have ductility, energy absorption capacity and is effective for crack control[1, 2]. FRCC is a mixture of concrete/cement mortar and short discontinuous fibers such as steel, glass, carbon and polymer fibers such as polyethylene, polypropylene, and polyvinyl alcohol. By incorporating fibers, typically up to a volume fraction of two percent, the brittleness of concrete is reduced[3]. At these relatively low fiber volume fractions, the contribution of fibers is mostly apparent in the post-cracking response, represented by an increase in post-cracking ductility, due to the work associated with pullout of fibers bridging a failure crack[4].

In tension, FRCC with relatively low fiber volume fractions of until 3% exhibit what is known as quasi-brittle behavior, that is the gradual decay of tensile stress (strain-softening) beyond the first cracking strength. The first cracking strength, similar to that of unreinforced mortar, corresponds to the tensile strength of the material[5]. In compression, adding fibers to a concrete matrix do not significantly improve its compressive strength however the strain at peak stress is increased by the presence of any type of fibers[4].

Engineered cementitious composites (ECC) is a class of FRCC. Its most remarkable feature is its enhanced tensile property; strain hardening occurs in tension after the first cracking strength has been reached with multiple micro-cracks instead of a single failure crack. The rising stress is accompanied by increasing strain, thus achieving a stress-strain curve with shape similar to that of a ductile metal. The compressive strength of ECC is not significantly higher than FRCC but the compressive strain capacity is approximately double than that of FRCCs[6]. ECC uses only fine aggregates in the mix to control the fracture toughness of the composite[7]. The lack of course aggregates in the mix results in a low composite elastic modulus. Designed based on micromechanics considerations, the fiber, cementitious matrix, and fiber/matrix interface must be of a correct combination to attain the unique properties of ECC[6].

Previous investigations have confirmed the positive effects of using FRCC for structural members subjected to cyclic loading conditions. These include the work of Filiatrault *et al.* wherein steel fiber reinforced concrete was used in beam-column joints[8]. They found that the presence of steel fibers in the joint increased the shear strength and can diminish the requirements for closely spaced ties. Daniel and Loukili examined the effect of longitudinal steel

ratio and steel fiber length on high-strength concrete beams under alternate cyclic bending[9]. They found that due to the presence of fibers, cracking is delayed at the pre-peak stage and the number and length of cracks were reduced. However, at the post-peak stage, ductility was not improved with the presence of fibers due to the severe bond deterioration between longitudinal bars and the composite.

Fischer and Li studied the effect of ECC on the unilateral reverse cyclic response of small-scale cantilever beam-columns[10]. An improvement in composite disintegration caused by a reduction in ECC spalling and crushing as well as a reduction of transverse steel reinforcement requirements were observed. Saiidi *et al.* investigated the effect of incorporating shape-memory alloys (SMA) and ECC on model columns subjected to simulated seismic loads[11]. Use of SMA bars reduced permanent displacements while use of ECC substantially reduced damage in the plastic hinge. Furthermore, the combination of SMA and ECC led to larger drift capacity as compared to the conventional steel reinforced concrete column.

As part of an effort to achieve better understanding on the use of FRCCs for improved seismic performance of bridge columns, bilateral cyclic loading experiments have been conducted. In particular, columns with SFRC and ECC were investigated. The columns considered have larger dimensions compared to small-scale columns previously tested by other researchers.

2. EXPERIMENTAL PROGRAM

(1) Specimen Properties

To investigate the structural response of flexural members with FRCC on potential plastic hinge region, three column specimens were constructed. The first is a conventional reinforced concrete, referred herein as RC. The second incorporated steel fiber reinforced concrete in the plastic hinge region, referred herein as SFRC. The third integrated engineered cementitious composites using polypropylene fibers in the plastic hinge, referred herein as polypropylene fiber reinforced concrete (PFRC). The columns are 1/4.5 scaled models of a prototype column. The columns were geometrically identical with square cross-section dimensions of 400mm x 400mm with rounded corners and an effective height of 1680 mm. Shear-span ratio (cantilever height to column width) is 4.2. Details of the specimens are shown in **Fig. 1.**

The specimens, designed based on the Japan Specifications of Highway Bridges[12], were designed to have the same flexural capacity and were designed as columns with concrete without considering differing properties of the FRCC. Concrete with higher than standard nominal compressive strength f'c of 60 MPa was used for the RC column. The nominal compressive strength of SFRC is 60 MPa while PFRC is 40MPa. SFRC and PFRC were used only from the footing up to a height of 600mm from the column base to minimize the cost. This height is three times the estimated plastic hinge length of one-half the column width[12] corresponding to 200mm to avoid failure at the SFRC/PFRC-concrete interface. Above this height, regular concrete was used.

Ready-mixed concrete with a water-cement ratio of 35% and maximum aggregate size of 13 mm was used. High-range water reducing admixtures and admixtures to enhance the workability of the mix were added. The measured compressive strength at the day of the loading test, determined using the average of three standard 100mm by 200mm cylinders, is 55 MPa with a strain at peak of 0.46%.

SFRC was made by combining the ready mixed concrete, with properties earlier mentioned, with 1.0% volume of steel fibers with hooked ends. The steel fibers were made from cold drawn wires and have diameter of 0.55mm and length of 30mm. Other relevant properties of the steel fibers are summarized in **Table 1.** Admixtures were also used during casting to enhance the fresh properties of the mix. The measured cylinder compressive strength of SFRC is 63 MPa with a strain at peak of 0.49%.

PFRC was made by combining high-strength cement mortar, fine aggregates (maximum grain size of 0.30mm), water, and 3% volume of polypropylene fibers which is equivalent to 1.5% fiber by weight. The polypropylene fibers are monofilament fibers with diameter of 42.6μm and length of 12mm[13]. Other important properties are shown in **Table 1.** Superplasticizers were also added to improve the workability of the mix. The measured cylinder compressive strength of PFRC is 38 MPa with a stain at peak of 0.54%.

The longitudinal steel reinforcement ratio and tie reinforcement ratio were identical in all specimens. Longitudinal reinforcement consisted of 36-10mm diameter deformed bars with nominal yield strength of 685MPa (SD685) resulting in a reinforcement ratio of 1.70%. The actual yield strength of longitudinal reinforcements is 710MPa at 0.4% strain. Tie reinforcement consisted of 6mm diameter deformed bars with nominal yield strength of 345 MPa (SD345) having 135° bent hooks. The actual yield strength of tie reinforcements is 363 MPa at 0.2% strain. Ties were spaced at 45mm (ρ_s = 0.70%) within 600mm height from the base and at 50mm spacing above (ρ_s = 0.60%). Concrete cover of 35mm was provided in all columns.

(2) Test set-up and loading protocol

The quasi-static cyclic loading experiment was conducted under displacement control. A constant axial load of 183 KN corresponding to 1.20 MPa axial stress in the plastic hinge was applied simultaneously with a bilateral displacement. The applied displacement is a circular loading orbit that increases at one half of the drift ratio. Drift ratio is defined as the column top lateral displacement divided by the effective height (height from the center of the lateral actuator to the top of footing). The

column was first loaded in the South (S) direction until 0.5% drift, then loaded three times by the circular orbit, then finally unloaded in S direction until the rest position (**Fig. 2**). Due to some problems with the lateral actuator system, a phase lag of 12.6° occurred between the North-South (NS) and East-West (EW) displacement components resulting to an elliptical loading orbit with the semimajor axis along the NE-SW direction.

The specimen footings were designed to be strong to avoid damage, minimize deformation and to avoid rocking. They were anchored to the test platform using four PC bars with 250kN prestressing force each.

A total of 70 channels per column were used to record three actuator forces, three actuator displacements, 10 linear variable differential transducers (LVDT) for translation/rotation/curvature measurements, 18 tie bar strains, and 36 longitudinal bar strains. Single electric resistance strain gages were used to monitor strains in tie and longitudinal bars at specific locations.

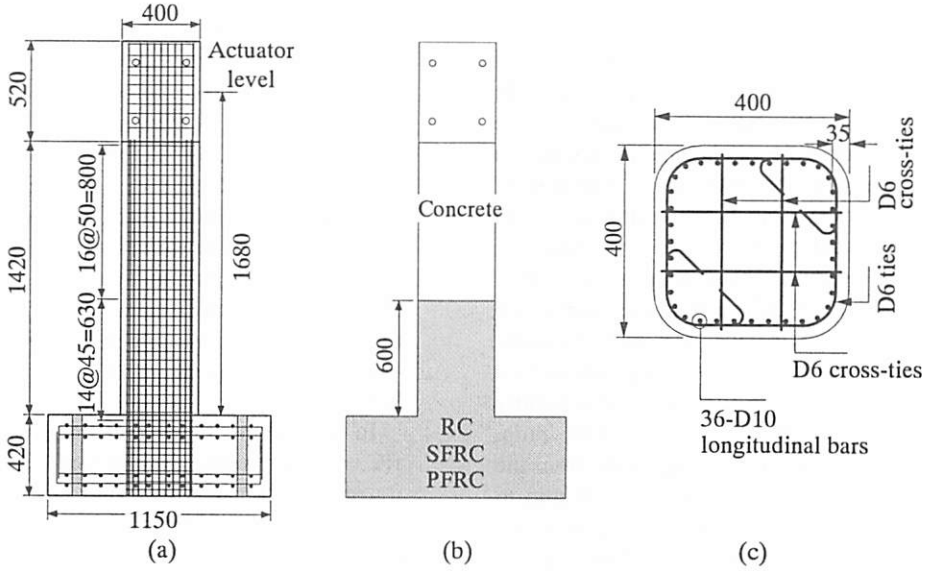

Fig. 1 Specimen configuration and details: (a) reinforcement detail, (b) concrete/composite property, and (c) cross-section

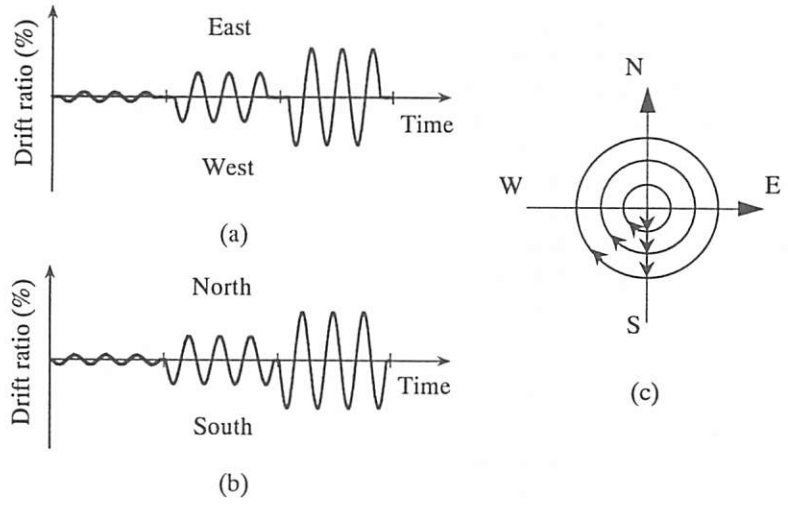

Fig. 2 Loading scheme: (a) East-West component, (b) North-South component, and (c) circular displacement orbit

Table 1 Properties of fibers used

Fiber type	Steel	Polypropylene
Tensile strength (MPa)	1100	482
Young's modulus (GPa)	210	5.0
Specific gravity	7.85	0.91

3. EFFECT OF FIBERS ON COLUMN CYCLIC RESPONSE

(1) Column Damage

Fig. 3 shows the damage propagation at the S-face of RC column. As observed from the experiment, damage was more severe in the SW-NE axis because of the elliptical displacement orbit hence damage at this face is shown. The concrete cover started to spall at the base of the SW corner at 2% drift ratio. At 3% drift ratio, cover concrete completely spalled-off within a height of 150mm from the base at the SW corner until the middle of S face, and at a height of 50mm from the base at the NE corner. Spalled concrete size was approximately 50mm and larger. At 4% drift ratio, two longitudinal bars were exposed at the SW corner which subsequently buckled at a height of 75mm. At 4.5% drift ratio, extensive spalling of cover concrete progressed from the corners to the four faces within a height of 100 mm to 250 mm from the base. Core concrete crushing was also observed from the NW corner to SE corner. Loading was terminated at this drift due to core concrete crushing and rupture of 14 (39%) longitudinal bars.

In SFRC column, cracking initiated at the base of SW and NE corners with hairline cracks at 2% drift ratio (**Fig. 4**). At 3% drift ratio, crushing of SFRC cover occurred at the SW corner then spread out to other faces at a height of 50 mm from the base. Crushed SFRC cover size was approximately 20 mm and smaller. At 4% drift ratio, at the SW corner, crushed material from inside which may be from cover and core comes out while the cover is not completely removed due to the steel fibers which hold the SFRC cover together. At the second cycle of 4% drift, four (11%) longitudinal bars ruptured as ascertained from the splitting sound heard. At 4.5% drift ratio, longitudinal bars and ties at 60 mm and 105 mm height from the base at the W face were exposed due to loss of SFRC cover. At the end of this drift ratio, 12 (33%) longitudinal bars ruptured. Total bars which ruptured are 16 (44%). Loading was also terminated at this drift due to rupture of majority of longitudinal bars.

In PFRC column, cracking also initiated at the base of the SW corner with hairline cracks at 2% drift ratio (**Fig. 5**). At 3.5% drift ratio, long, flexural cracks were observed at a height of 600 to 1100 mm from base at an approximate spacing of 100-150 mm at all faces. ECC cover spalling and crushing, however, were not observed. At 4% drift ratio, the number of short flexural cracks in the column faces increased within 200mm from the base. In addition, the tendency of the longitudinal reinforcement to buckle resulted in formation of longitudinal splitting cracks at the SW and NE corner within 300mm from the base. At the third cycle of 4% drift ratio, one (3%) longitudinal bar ruptured. Further increasing the displacement to 4.5% drift ratio, longitudinal cracks at the corners widened to about 6mm to accommodate the lateral expansion of the plastic hinge. Nevertheless, cover concrete spalling was not observed and longitudinal bars and ties were also not exposed. At the end of this drift ratio, 11 (30%) longitudinal bars ruptured. Total bars which ruptured are 33%. Loading was also terminated at this drift due to rupture of longitudinal bars.

In contrast to a brittle concrete spalling and cracking in RC column, the presence of steel fibers in SFRC column transformed the cracking into a less brittle failure. The presence of steel fibers delayed crack propagation and prevented further crack opening through the bridging action of fibers across cracks. Reverse cyclic loading caused severe cover concrete compression failure within 150mm height from the base for RC column exposing longitudinal bars and two tie layers while cover compression failure occurred within 50mm height from the base for SFRC column. This is the effect of the higher compression strains that can be sustained by the SFRC composite due to the confining effect of fibers compared to concrete.

As shown in **Fig. 6**, the extent of damage varied significantly among the three columns. Whereas extensive cover and core damage was evident in RC column and limited cover spalling in SFRC column, damage in PFRC column was restricted to relatively minor cracks. Similar to SFRC, the presence of polypropylene fibers in PFRC delayed crack propagation and resulted to the formation of numerous small, thin, flexural cracks. The column also benefited from the higher compression strain of the PFRC composite, providing resistance against cover spalling even at large displacements.

(2) Longitudinal and tie-bar strains

In the cyclic loading test, damage was severe in the SW and NE corner. Hence, because of space limitations focus will be on strains measured at the SW corner. Note that measurement of bar strains is difficult due to damage

of strain gages, thus only reliable measured data will be shown.

Fig. 7 shows strain distribution of longitudinal bar 218mm from the column base. This height is slightly above the anticipated plastic hinge region. With a yield strain of 4,000μ, the longitudinal bars of all three columns yielded in tension at 1.5% drift ratio and that the strains were over 12,000μ at 3% drift. Variation of longitudinal bar tensile strains among the three columns was not significant. However, bar compression strains were largest in PFRC column. For example, at the first cycle of 3% drift, bar compression strain of PFRC column was 6,400μ which is 43% larger than RC column.

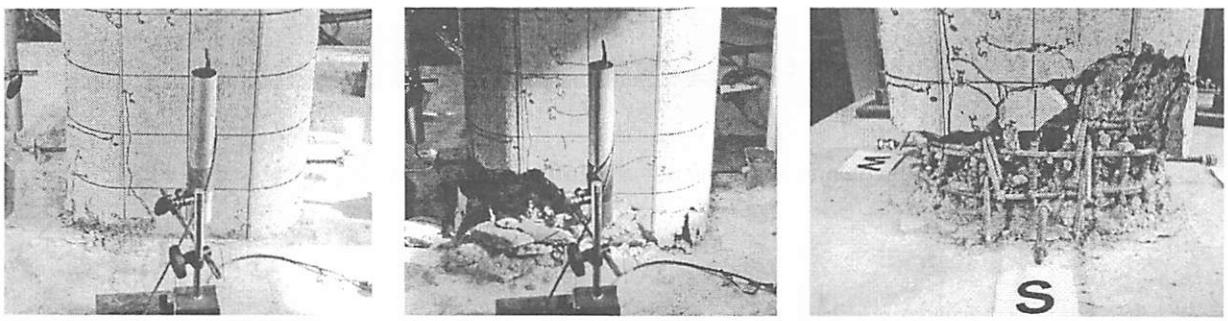

(a) (b) (c)

Fig. 3 Damage of RC column at S-face: (a) 2% drift, (b) 3% drift, and (c) 4.5% drift

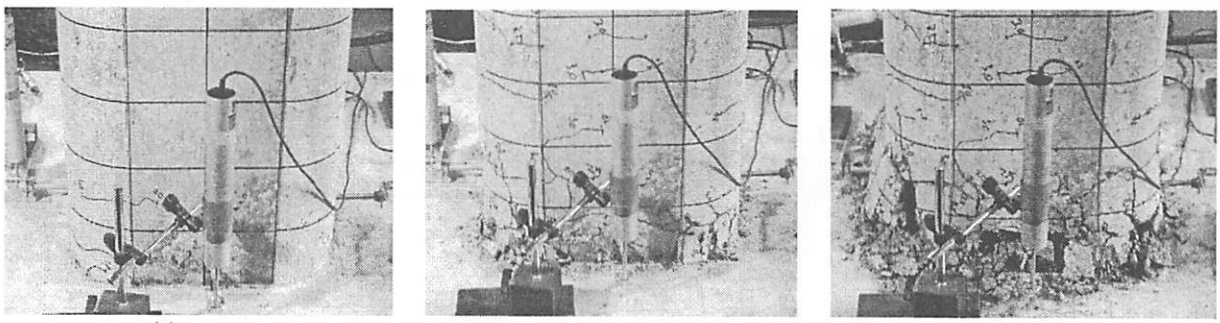

(a) (b) (c)

Fig. 4 Damage of SFRC column at S-face: (a) 2% drift, (b) 3% drift, and (c) 4.5% drift

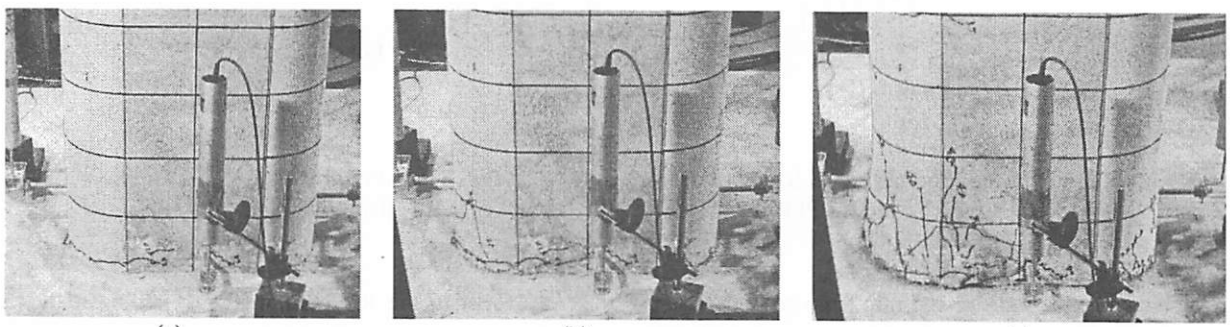

(a) (b) (c)

Fig. 5 Damage of PFRC column at S-face: (a) 2% drift, (b) 3% drift, and (c) 4.5% drift

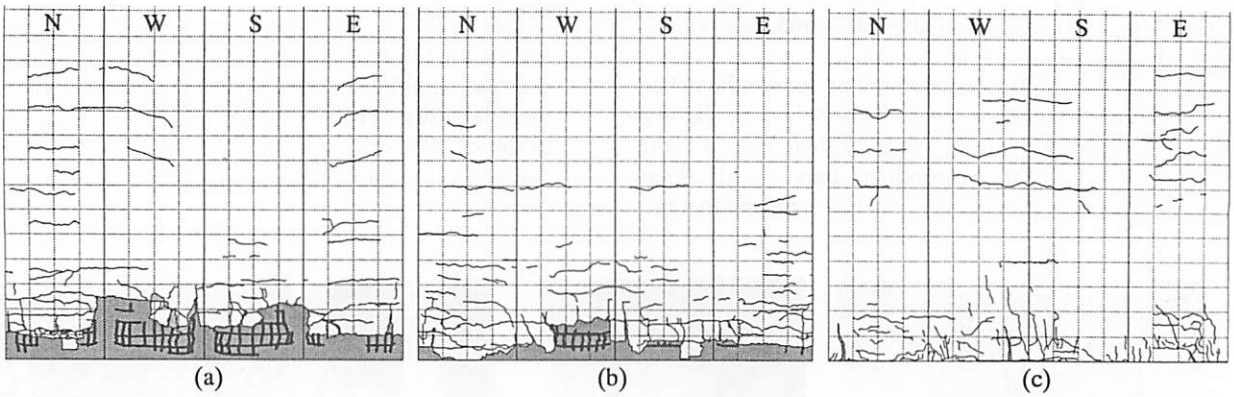

Fig. 6 Damage of columns at the end of 4.5% drift loading: (a) RC, (b) SFRC, and (c) PFRC

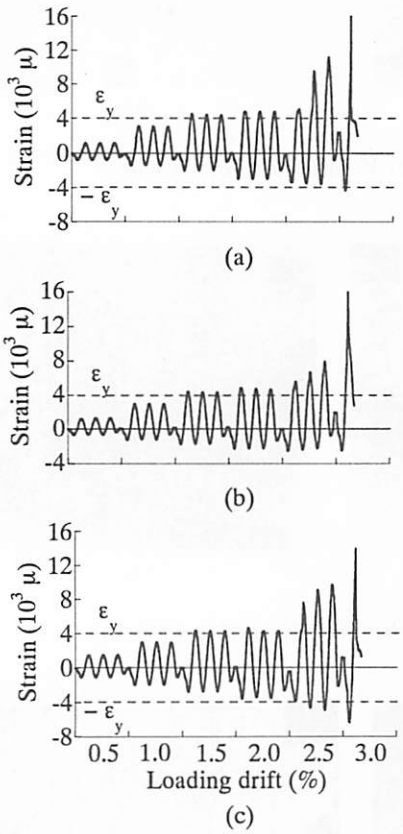

Fig. 7 Strain of longitudinal bar at SW corner: (a) RC, (b) SFRC, and (c) PFRC

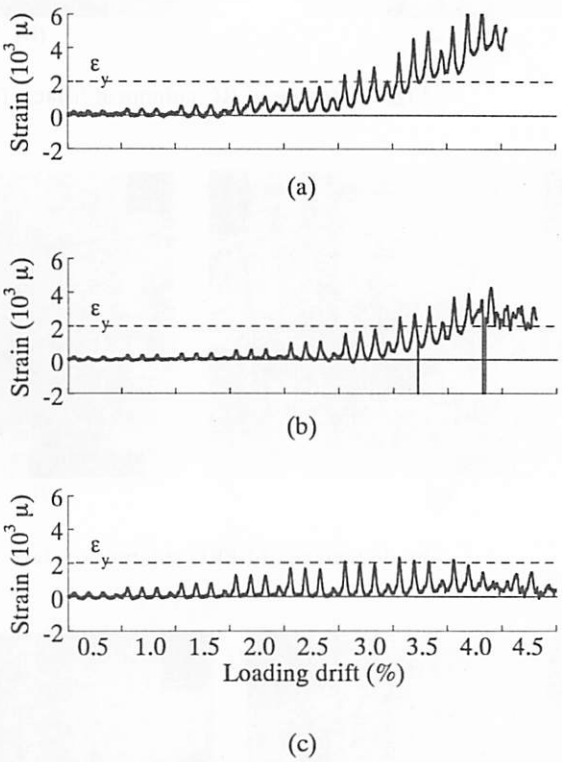

Fig. 8 Strain of tie bar at SW corner: (a) RC, (b) SFRC, and (c) PFRC

Strain of tie bar located 105 mm from column base is shown in **Fig. 8**. Tie bar in the RC column has already yielded while tie bars in SFRC and PFRC column have strains nearly equal to the yield strain at 3% drift. At 4% drift, tie strains increased to as high as 6,000μ in RC column and 4,000μ in SFRC column however tie strains in PFRC column was only about 2,000μ. As mentioned earlier, two longitudinal bars at the SW corner buckled at 4% drift in the RC column. The yielding of ties at the SW corner is due to this local buckling of longitudinal bars. At 4% drift, it is likely that several longitudinal bars buckled at SFRC and PFRC column based on the occurrence of longitudinal splitting cracks and rupture of bars which is related to the tie strains. The measured tie strains in SFRC and PFRC column were less compared to that of RC column. Hence, a reduction of tie strains

with the use of SFRC or PFRC can result to reduced transverse reinforcement requirements. A similar observation was reported by Filiatrault *et al.*[8] for SFRC columns and by Fischer and Li[10] for PFRC columns.

(3) Force-displacement hysteresis

Figs. 9 and **10** show the lateral force vs. top lateral displacement hysteresis of the columns in the EW and NS direction, respectively. Taking the average of the maximum restoring force in the push and pull direction, then the average in the EW and NS direction, **Table 2** shows that RC column reached a maximum strength of 163 KN. The measured response of RC column showed a stable and ductile response until 4% drift ratio (**Fig. 9a** and **10a**). The restoring force deteriorated to 86% of its maximum strength at 4.5% drift ratio due to compression failure of core concrete and extensive buckling as well as rupture of longitudinal bars.

SFRC column similarly showed a stable and ductile response until 4% drift ratio with an average maximum strength of 171 KN (**Fig. 9b** and **10b**) which is about 5% higher than RC column due to the higher compressive strength of SFRC. The restoring force deteriorated at 4.5% drift due to rupture of 44% of longitudinal bars reducing the restoring force to 59% of its maximum strength.

PFRC column attained an average maximum strength of 158 KN which is 3% and 8% lower compared to RC and SFRC column, respectively, due to the lower compressive strength of PFRC. The difference in the flexural strength of the three columns however is not significant. PFRC column demonstrated a stable and ductile response until 4% drift ratio (**Fig. 9c** and **10c**). Although cover spalling and crushing was not observed, the restoring force decreased to 81% of its maximum strength at 4.5% drift due to rupture of 33% of the longitudinal bars.

Comparison of the lateral force vs. lateral displacement hystereses of the columns do not show the effect of SFRC and PFRC on improving flexural strength and ductility of the specimens. Although SFRC and PFRC reduced cover spalling and core crushing providing lateral stability for the longitudinal bars to endure cyclic inelastic deformations, failure of the columns was governed by rupture of longitudinal bars.

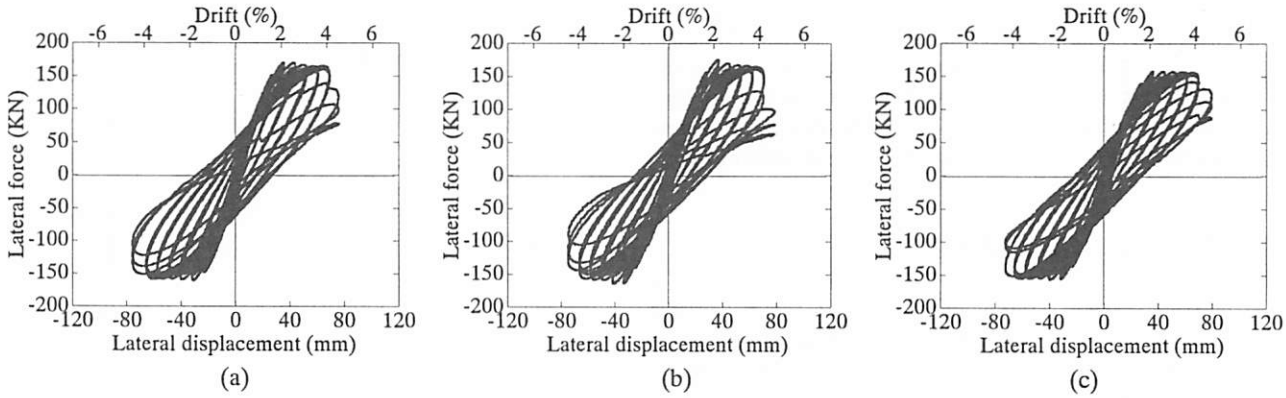

Fig. 9 Lateral force vs. lateral displacement hysteresis (EW direction): (a) RC, (b) SFRC, and (c) PFRC

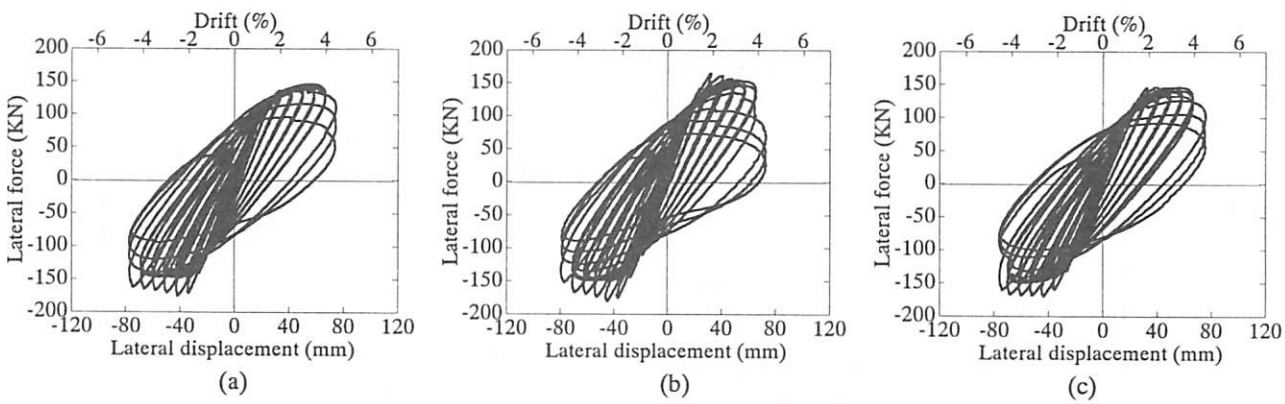

Fig. 10 Lateral force vs. lateral displacement hysteresis (NS direction): (a) RC, (b) SFRC, and (c) PFRC

Table 2 Flexural strength comparison for RC, SFRC and PFRC column

Specimen	Maximum Flexural Strength (KN)						
	EW-direction			NS-direction			Average of (1) & (2)
	+	-	(1) Average	+	-	(2) Average	
RC	169.7	160.7	165.2 (100%)	145.7	175.8	160.8 (100%)	163.0 (100%)
SFRC	174.9	164.4	169.7 (103%)	164.7	180.6	172.7 (107%)	171.2 (105%)
PFRC	158.1	156.8	157.5 (95%)	145.7	170.5	158.1 (98%)	157.8 (97%)

4. CONCLUSIONS

To clarify the effect of fiber reinforced cement composites on the cyclic response of bridge columns, bilateral cyclic loading experiments were conducted. Based on the results presented, the following conclusions can be deduced:

1) The use of fiber reinforced cement composites (FRCC) such as steel fiber reinforced concrete (SFRC) and polypropylene fiber reinforced concrete (PFRC) reduced cover concrete spalling and crushing on column plastic hinges.
2) Strains of ties in SFRC and PFRC columns were less compared to that of RC column. This can result in reduced tie reinforcement requirements.
3) Column flexural strength and ductility was not improved even with the presence of fibers. Although SFRC and PFRC reduced cover concrete spalling and crushing providing lateral stability for the longitudinal bars to endure cyclic inelastic deformations, column failure was governed by rupture of longitudinal bars.

ACKNOWLEDGEMENTS

This study was conducted as part of the E-Defense Bridge Project of the National Research Institute for Earth Science and Disaster Prevention (NIED). The authors sincerely thank Hiromichi Ukon (former research fellow of NIED) and Takayoshi Hirata (Obayashi Corp.) for the material technical support. Finally, Hiroshi Matsuzaki, Assistant Professor of Tokyo Institute of Technology and students Guilian Quan, Huang Szu-chia, Yuji Kumagai, Wang Jing, Zhang Rui, Keisuke Ohta and Syota Ichikawa are gratefully acknowledged for their assistance in executing the experiments.

REFERENCES

1) Shah, S. P. and Naaman, A. E.: Mechanical properties of glass and steel fiber reinforced mortar. *ACI Journal, Proceedings*, Vol. 73, No. 1, pp. 50-53, 1976.
2) Parra-Montesinos, G.: High-performance fiber reinforced cement composites: an alternative for seismic design of structures, *ACI Structural Journal*, Vol. 102, No. 5, pp. 668-675, 2005.
3) Tjiptobroto, P. and Hansen, W.: Tensile strain hardening and multiple cracking in high-performance cement-based composites containing discontinuous fibers, *ACI Materials Journal*, Vol. 90, No. 1, pp. 16-25, 1993.
4) Fanella, D. and Naaman, A.: Stress-strain properties of fiber reinforced mortar in compression, *ACI Journal*, July-August, pp. 475-483, 1985.
5) ACI Committee 544. Design considerations for steel fiber reinforced concrete, *ACI Structural Journal*, September-October, pp. 563-580, 1988.
6) Li, V.: Engineered cementitious composites (ECC) – tailored composites through micromechanical modeling, *Fiber Reinforced Concrete: Present and the Future*, N. Banthia, and A. Mufti, eds., Canadian Society of Civil Engineers, Montreal, pp. 64-97, 1998.
7) Li, V., Mishra, D. and Wu, H.: Matrix design for pseudo-strain-hardening fibre reinforced cementitious composites, *Materials and Structures*, Vol. 28, pp. 586-595, 1995.
8) Filiatrault, A., Pineau, S. and Houde, J.: Seismic behavior of steel-fiber reinforced concrete interior beam-column joints, *ACI Structural Journal*, Vol. 92, No. 5, pp. 1-10, 1995.
9) Daniel, L. and Loukili, A.: Behavior of high-strength fiber reinforced concrete beams under cyclic loading, *ACI Structural Journal*, Vol. 99, No. 3, pp. 248-256, 2002.
10) Fischer, G. and Li, V.: Effect of matrix ductility on deformation behavior of steel-reinforced ECC flexural members under reversed cyclic loading conditions, *ACI Structural Journal*, Vol. 99, No. 6, pp. 781-790, 2002.
11) Saiidi, M., O'Brien, M., and Sadrossadat-Zadeh, M.: Cyclic response of concrete bridge columns using superelastic nitinol and bendable concrete, *ACI Structural Journal*, Vol. 106, No. 1, pp. 69-77, 2009.
12) *Japan Road Association Specifications for Highway Bridges*, Maruzen, Tokyo, 2002.
13) 平田 隆祥,川西 貴士,岡野 素之,渡辺 哲.:ポリプロピレン短繊維を用いた高じん性セメント系材料の物性と構造性能に関する基礎的検討, コンクリート工学年次論文集, Vol. 31, No.1, pp. 295-300, 2009.